energies

MDPI

Article

Comparison of Evaporite-Related Source Rocks and Implications for Petroleum Exploration: A Case Study of the Dongying Depression, Bohai Bay Basin, Eastern China

Yong Chen [1,2,*], Yun Han [1], Pengfei Zhang [3], Miao Wang [1,*], Yibo Qiu [3], Xuelei Zhu [1] and Xuejun Zhang [3]

[1] School of Geosciences, China University of Petroleum, Qingdao 266580, China; hy_helen1991@163.com (Y.H.); zxl13151719@163.com (X.Z.)
[2] Laboratory for Marine Mineral Resources, Qingdao National Laboratory for Marine Science and Technology, Qingdao 266071, China
[3] Shengli Oilfield Company, SINOPEC, Dongying 257015, China; zpf0725@126.com (P.Z.); qiuyibo77@163.com (Y.Q.); zhangxuejun338.slyt@sinopec.com (X.Z.)
* Correspondence: yongchenzy@upc.edu.cn (Y.C.); 20200081@upc.edu.cn (M.W.)

Abstract: The Dongying Depression (Bohai Bay Basin, eastern China) was widely filled with evaporite (anhydrite and halite) layers during the Paleogene period, especially the middle of the fourth member of the Shahejie Formation (Es_4). Most evaporite layers are interbedded with mudstone strata. The strata of Es_4 are divided into three sections, referred to as the upper layers, evaporite layers, and lower layers, respectively. The analysis of elemental concentrations, elemental ratios, and Pr/Ph suggests that the lower layers were deposited in an intermittent saline lake environment within a relatively dry climate. The evaporite layers were formed in a highly saline lake environment, whereas the upper layers were formed in a brackish-saline to fresh-water environment. Organic matter (OM) abundance indices, including total organic carbon (TOC), chloroform extracts, total hydrocarbon content (HC), hydrocarbon generation potential ($S_1 + S_2$), and OM type, show that the source rock potential for petroleum generation in the upper layers is best, that in the evaporite layers is fair, and in the lower layers it is poor. Carbon isotopes ($\delta^{13}C$) of hydrocarbons in the evaporite and lower layers were heavier than those in the upper layers. Thermal maturity parameters show that the thermal evolution process of OM in the upper layers was faster where evaporite were present compared with evaporite-free areas, while the thermal evolution of OM in the lower layers was slower in these regions. The high thermal conductivity of evaporites may have accelerated the thermal evolution of source rocks in upper layers and allowed hydrocarbon generation at a shallower burial depth. This resulted in the earlier appearance of the petroleum generation window compared to in evaporite-free areas. Meanwhile, the thermal evolution of OM in the lower layers was restrained, and consequently the hydrocarbon generation window was widened, which implies the potential for petroleum exploration in deep strata under the evaporite sequence. This is a common phenomenon in evaporite-bearing basins, according to previous and present studies.

Keywords: evaporites; source rock; hydrocarbon generation potential; thermal evolution; T_{max}; TOC

check for updates

Citation: Chen, Y.; Han, Y.; Zhang, P.; Wang, M.; Qiu, Y.; Zhu, X.; Zhang, X. Comparison of Evaporite-Related Source Rocks and Implications for Petroleum Exploration: A Case Study of the Dongying Depression, Bohai Bay Basin, Eastern China. *Energies* **2023**, *16*, 5000. https://doi.org/10.3390/en16135000

Academic Editor: Nikolaos Koukouzas

Received: 26 April 2023
Revised: 20 June 2023
Accepted: 21 June 2023
Published: 28 June 2023

Copyright: © 2023 by the authors. Licensee MDPI, Basel, Switzerland. This article is an open access article distributed under the terms and conditions of the Creative Commons Attribution (CC BY) license (https://creativecommons.org/licenses/by/4.0/).

1. Introduction

Recent reviews of more than 180 petroliferous basins around the world reveal that about 120 basins contain appreciable evaporite (i.e., anhydrite, gypsum or halite) strata [1–4]. Evaporite beds are widespread and common in petroleum-bearing basins, especially those with large oil and gas fields, such as the Scotian Shelf Basin [5], the Delaware Basin [6], the Persian Gulf Basin [7,8], the Southern Permian Basin, in NW Europe [9], the Gulf of Mexico Basin [10,11], the Red Sea Basin [12], the Aaiun Basin, NW Africa [13], the Dnieper-Donets Basin, Ukraine [14], the Qaidam Basin, western China [15–17], the Tarim Basin, NW China [18,19], and the Dongpu [20,21], Bonan [22], and the Dongying Depression of

the Bohai Bay Basin [23,24], eastern China. Thus, studies on the evaporites in hydrocarbon source rocks and their roles in affecting hydrocarbon generation have aroused broad research interest. Previous studies showed that evaporite beds have a close relationship with the generation and accumulation of petroleum [3,25,26]. Kirkland and Evans [25] proposed that organic matter (OM) concentrated in evaporitic strata has excellent hydrocarbon generation potential. Subsequent research corroborated that good source rocks can be formed in saline-lake depositional environments [15,16]. The presence of evaporite beds in sedimentary basins could modify the thermal profile, leading to situations in which the sediments stratigraphically below salt structures may be colder relative to those with no overlying salt [27–30]. In some cases, the strata above and below evaporites appear isolated, but may actually interact with each other through tectonic movement, the flow of fluids, and chemical reactions [18,29,31].

At present, major questions remain regarding the formation and distribution of evaporites, geochemical characteristics, and differences within the evaporite-related source rocks, and it is necessary to know their roles in affecting the hydrocarbon generation process. The fourth member of the Paleogene Shahejie Formation (Es_4) in the Dongying Depression, Bohai Bay Basin, hosts the most economically valuable hydrocarbon source rocks of eastern China, and this source rock contains widespread evaporite layers and shows that the OM abundance of source rocks formed in saline-lacustrine environments is higher compared to other lithologies [32]. Petroleum exploration in recent years has discovered oil and gas in the lower section of Es_4, showing that these source rocks have good hydrocarbon potential [33] and are ideal study objects for the above problems. Here, we conducted comparative studies of the geochemical characteristics of evaporite-related source rocks of Es_4 in the Dongying Depression, to understand their formation and evolution in the context of associated evaporite layers. Our study is helpful to deepen the understanding of the effect of evaporites within source rocks on hydrocarbon generation and expulsion processes.

2. Geological Setting

The Dongying Depression is located in the eastern Bohai Bay Basin, eastern China. It is an oil-rich, lacustrine sedimentary depression, and the area of exploration (~5700 km^2) around the depression contains >10 oil and gas fields. The Dongying Depression can be divided into seven secondary structural units, including the Northern Steep-Slope Belt, the Central Uplift Belt, the Minfeng Sag, the Lijin Sag, the Niuzhuang Sag, the Boxing Sag and the Southern Gentle-Slope Belt (Figure 1) [34,35]. The four sags are not only the sedimentary center of the basin, but also the host areas of the main source rocks. According to the drilling data from the Shengli Oilfield Company, China Petrochemical Corporation (SINOPEC), the Cenozoic strata of the Dongying Depression comprise the Paleogene Kongdian Formation (Ek), the Shahejie Formation (Es), the Dongying Formation (Ed), the Neogene Guantao Formation (Ng), the Minghuazhen Formation (Nm) and the Quaternary Pingyuan Formation (Qp), respectively, from bottom to top [36,37].

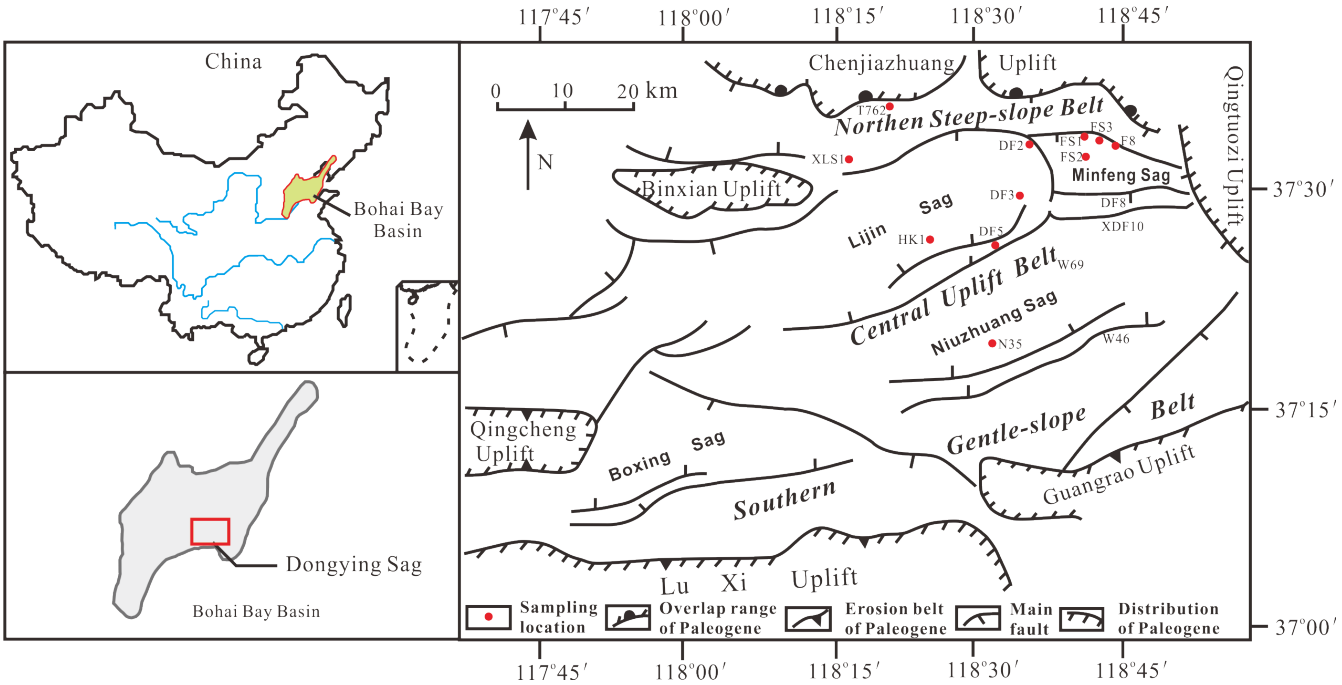


Figure 1. Map showing the location and regional tectonic characteristics of the Dongying Depression (modified from [38]).

There are four sets of evaporite beds in the Dongying Depression: one is in the Kongdian Formation (Ek) (not discussed in this paper), and the others are in the fourth member of the Shahejie Formation (Es_4). The upper submember of Es_4 (Es_{4U}) is one of the main hydrocarbon source rocks [39,40], and its lithofacies include calcareous shale, grey dolomitic mudstone, dark grey mudstone, calcilutite, and oil shale. These source rocks are widespread around the center of the Lijin and Boxing Sags. The lithofacies of source rocks in the upper part of the lower submember of Es_4 ($Es_{4L}{}^{upper}$) are dark grey shale, grey mudstone, calcilutite, evaporite beds with shale, dolomitic mudstone, and gypsum-bearing shale. At the base of the lower submember of Es_4 ($Es_{4L}{}^{lower}$), the lithofacies include the gypsum-bearing mudstone, grey green mudstone, and gypsum and halite-bearing mudstone. These source rocks of the Es_{4L} are mainly distributed in the Minfeng and Lijin Sags. Thus, the source rocks of $Es_{4L}{}^{upper}$ host the three sets of evaporite beds and are the main vertical intervals of evaporite layers. In this study, we took the $Es_{4L}{}^{upper}$ as a reference stratum, and the strata above and below this reference stratum in Es_4 are referred to as the upper layers and lower layers, respectively. The lithological section of the representative well FS1 is shown in Figure 2.

The drilling data showed that the first set of evaporite beds in the E_{S4L} is the thickest [36]. Laterally, evaporites are widespread in the Central Uplift Belt, to the north of the Dongying Depression. The evaporite beds are concentrated in the Northern Steep-Slope belt and the Central Uplift belt, and are exhibited around three sedimentary centers (Figure 3): the wells Haoke1 (HK1), Dongfeng1 (DF1), and Dongfeng8 (DF8). Additionally, the burial depth of strata in the northern slope is greater than that in the central uplift. In addition, the evaporite beds are interbedded with the mudstone beds in the $E_{S4L}{}^{upper}$, which indicates that both are syngenetic.

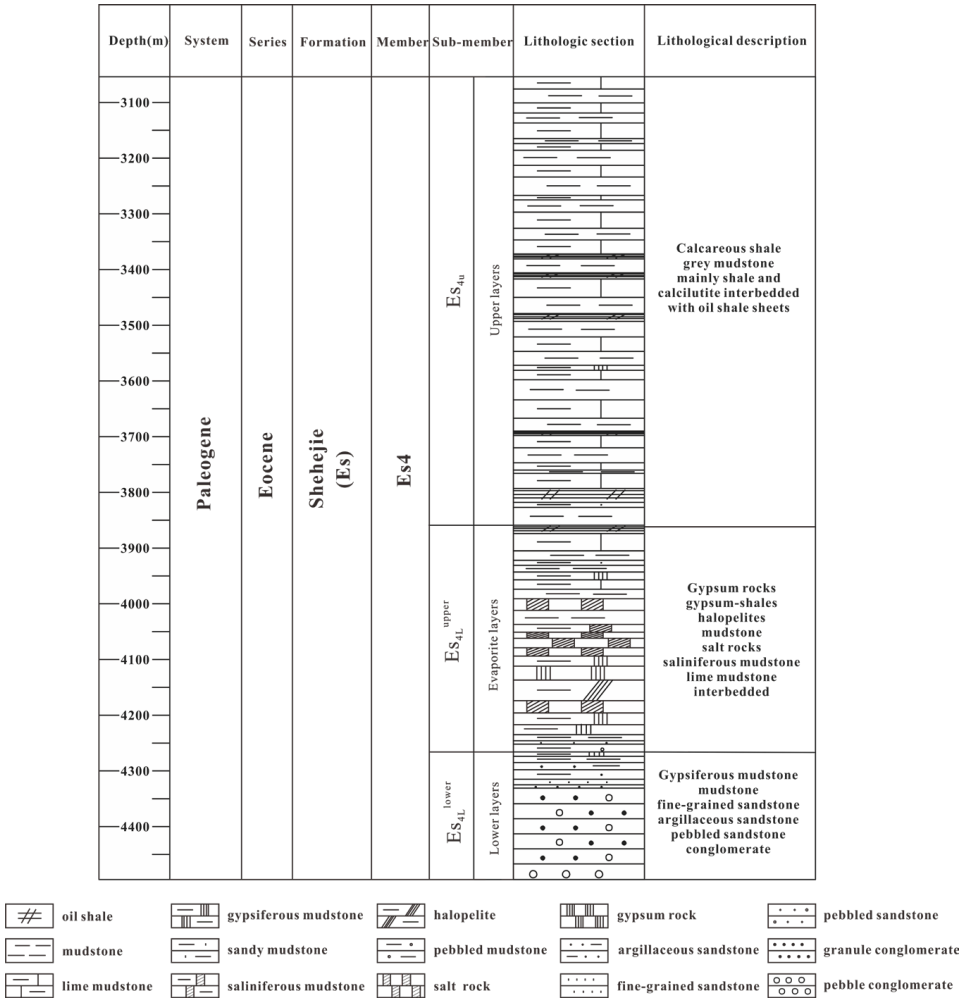


Figure 2. Lithological section of evaporite-related source rocks in Es_4 in the Dongying Depression (data from well FS1).

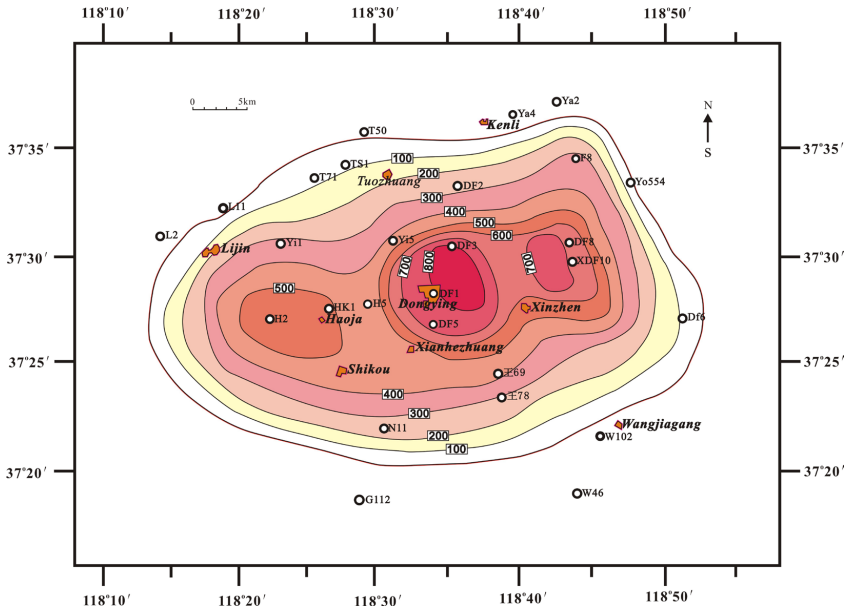


Figure 3. Map showing the isopach of evaporite beds of Es_4-Ek Formation in the Dongying Depression.

3. Analytical Methods

Considering the possible effects of facies variations and tectonic evolution, we chose the samples from one well or the same area to make each comparison, in order to avoid the possible effects. Most of our data were collected by the Institute of Geological Sciences of Shengli Oilfield Company. Major and trace elements (K, Na, Cu, Mg, Fe, Al, Mn, Ba, Sr, Zn, V, and Ni) with concentrations ranging from μg/L to g/L of 89 shale core samples from well HK1 were analyzed using Inductively Coupled Plasma Optical Emission Spectrometry (ICP-OES), conducted at the Formation Laboratory of the Institute of Geological Sciences of Shengli Oilfield Company. All other analyses (described below) were conducted at the Geochemistry Laboratory of the Institute of Geological Sciences. The vitrinite reflectance (R_o) of 30 samples was measured using UMSP-50 microphotometry; more than one hundred points were tested, and then the average was calculated for each sample. Kerogen analysis under the thin sections of 15 samples from the FS 2 well was performed using a DMRXP fluorescence microscope. Organic carbon contents of 17 shale samples from well FS1 were measured after removing carbonates. Total organic carbon content (TOC), T_{max} (temperature of maximum kerogen pyrolysate yield), residual soluble hydrocarbon (S_1), and pyrolysed hydrocarbon (S_2) of shale samples were measured with Rock-Eval pyrolysis 6.

Rock samples were powdered after removal of any superficial contamination. All of the samples were subjected to analysis with a Rock-Eval/TOC analyzer, and selected samples (considering the distribution samples in the upper, lower and evaporite layers) were then extracted in a Soxhlet apparatus with chloroform/ethanol (98:2, *v*/*v*) for 72 h. Asphaltene was precipitated by adding about 30 mL n-hexane and ultrasonic dissolution, which was maintained for 12 h. The extracts were fractionated on a neutral alumina chromatographic column into saturate, aromatic hydrocarbons, and a polar fraction, via sequential elution with *n*-hexane, toluene, and chloroform. For the quantitative determination of absolute concentrations of aliphatic and aromatic hydrocarbons, known amounts of standard compounds, 20R-5α14α17α (H)-d4-cholestane and d8-dibenzothiophene, were added to the concentrated extracts prior to fractionation.

Gas chromatography (GC) of saturated hydrocarbon fractions was performed on a Hewlett-Packard 5160 GC fitted with an SE54 fused silica column (25 m × 0.25 mm i.d.). The GC oven was initially set at 50 °C for 2 min, and then programmed to 300 °C at 4 °C/min. Gas chromatographic–mass spectrometric analyses (GC-MS) of saturated and aromatic hydrocarbon fractions were carried out on a Hewlett-Packard 5980 Mass Selective Detector (MSD) fitted with a 30 m × 0.25 mm i.d. HP-1 MS capillary column (with 0.25 mm film thickness). For analyzing saturated hydrocarbons, the GC oven was initially set at 50 °C for 2 min, programmed to 100 °C at 2 °C/min and then to 310 °C at 3 °C/min, and had a final holding time of 15 min. For analyzing aromatic hydrocarbons, the GC oven was initially set at 60 °C, programmed to 150 °C at 8 °C/min and then to 320 °C at 4 °C/min, and had a final holding time of 10 min. The mass spectrometer was operated in selected ion monitoring mode.

HCl at the concentration of 15% was used to remove carbonates from the powdered samples, and then the residual powder was wrapped with a tinfoil sheet. After that, the samples were analyzed for the carbon isotope composition of hydrocarbons using MAT251 Gas Isotope Ratio Mass Spectrometer with an error < 0.5%, and the PDB was used as standard [41].

4. Results

4.1. Inorganic Chemistry and Typical Elements Ratios

In order to avoid the effect of sedimentary facies variations, we analyzed the elemental ratios in the key exploration well HK1 (Figure 4) and investigated the sedimentary environment of Es_4. As well HK1 is located near the Central Uplift Belt, the burial depth of the strata (Es_4) is obviously less than that of well FS1. The results show that the concentrations and ratios of certain elements present cyclicity during the Es_4 deposition.

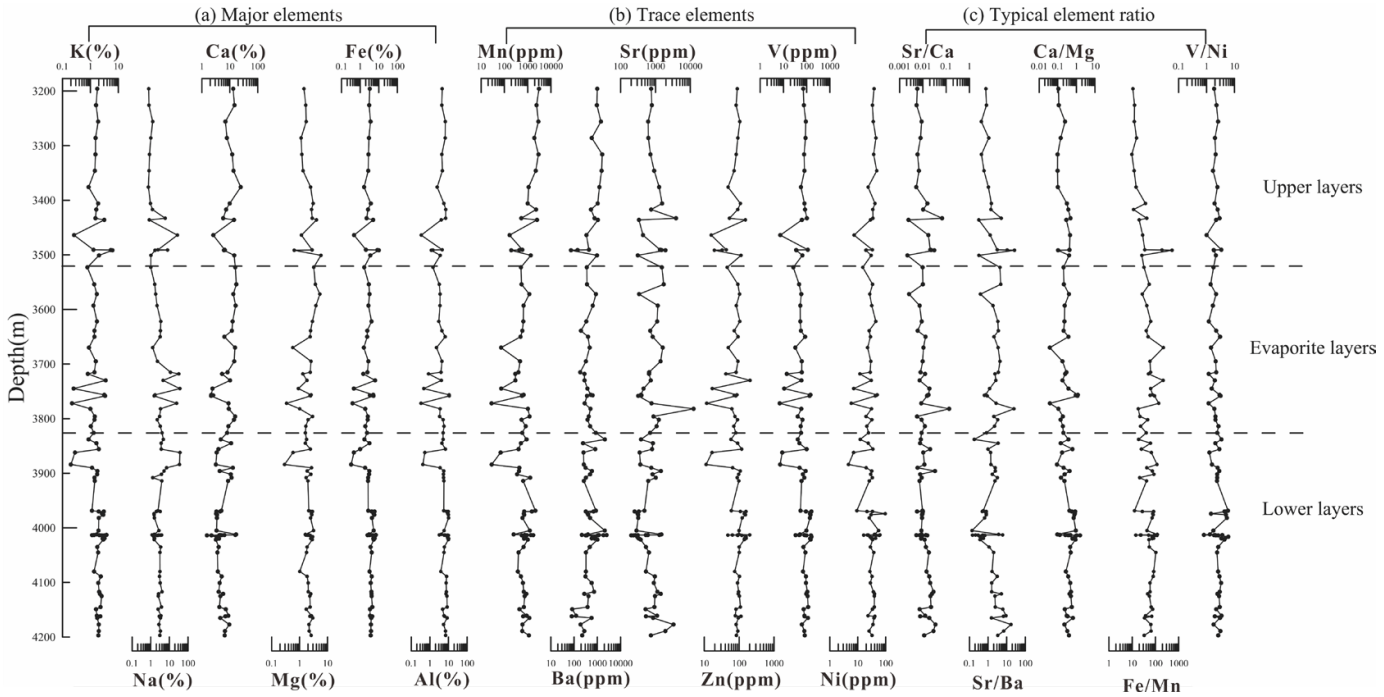


Figure 4. Major elements, trace elements, and typical elemental ratios of the upper, evaporite, and lower layers in the Dongying Depression. The samples were collected from well HK1 because it is the key well for scientific story. (**a**) Shows the major elements' change with depth; (**b**) shows the trace elements' change with depth; (**c**) shows the typical element ratios' change with depth.

From the bottom (4200 m) to the center (4000 m) of the lower layers, Ca, Sr, and the Sr/Ba ratio displayed an obviously decreasing trend, Ba and the Ca/Mg ratio displayed an obviously increasing trend, and other elements remained stable. There was a remarkable change for all major elements at the top of the lower layers. K, Ca, Mg, Fe, and Al showed a decreasing trend, coexisting with the increasing trend for Na. The average of Fe concentration in the bottom of the lower layers was about 3.9 wt%, increasing to 4.8 wt% towards the middle of the lower layers, and then showed an obvious decrease towards the top of the lower layers, reaching a minimum value of 0.3 wt%.

Most element contents showed obvious fluctuations in the evaporite layers. The evaporite layers with anhydrite and halite were mainly composed of Ca and Na. The concentrations of certain major elements (K, Fe, Al) and trace elements (Mn, Zn) showed decreasing trends in bulk, while Na, Ca, and Sr showed increasing trends. The variation and cyclicity of elemental contents at the bottom of evaporite layers was pronounced. Trends in K, Mg, Fe, and Al concentrations were correlated, whereas Na showed the opposite trend. For trace elements, trends in Mn, Zn, V, and Ni were consistent. The Sr/Ba and Sr/Ca ratios showed consistent relative variation, while the Ca/Mg ratio displayed the contrasting trend to Sr/Ba and Sr/Ca in the evaporite layers.

Elemental concentrations and ratios in the upper layers showed significant differences relative to those in the evaporite layers. The contents of Na, Mg, and Sr were relatively low, while those of Ca, Fe, Al, Mn, Ba, and V were higher in the upper layers, and Sr/Ba, Sr/Ca, and Fe/Mn ratios were also relatively low, especially the Fe/Mn ratio, showing an obvious decreasing trend upwards in the upper layers. The upper layers showed only slight variations in most concentration and ratio values, except the part near the bottom of this section.

4.2. Geochemical Characteristics of Source Rocks

Evaporite beds are widespread in the Central Uplift Belt to the north of the Dongying Depression. Well FS1 in the Mingfeng Sag is representative of the deep lithology profile

of the studied area (Figure 5). A statistical analysis on the geochemical characteristics (including the type of OM, TOC, and chloroform extracts of source rock) of this section was performed (Figure 5).

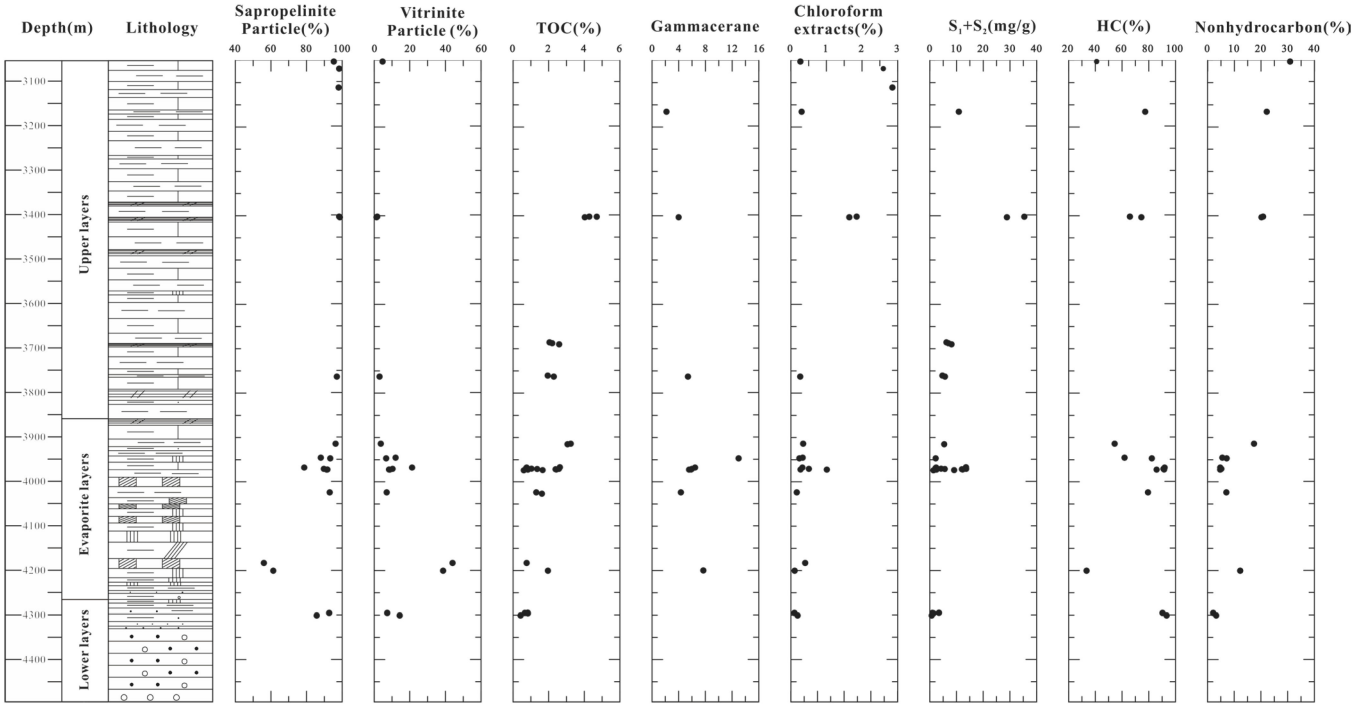


Figure 5. Organic geochemical characteristics in a section of evaporite-related source rocks in Es_4 in the Dongying Depression. The samples were collected from well FS1.

4.2.1. Kerogen Type

The kerogen types were determined according to the method reported by Tissot and Welte [42]. The results of maceral analyses (Figure 5) showed that the kerogen of source rocks in upper layers were sapropelinite and consisted mainly of type I kerogen. The kerogen of source rocks in the evaporite layers was mainly sapropelinite, with little vitrinite. According to the calculation method proposed by Li and Lu [43], the numerical kerogen type index (NKTI) was 62.7–93.6 and the kerogen was mainly type I, with lesser amounts of type II_1 for studied samples. The kerogen type II_1 was determined by the ratio of H/C and O/C, with a range of 1.2–1.45 and 0.1–0.15, respectively [44]. The vitrinite content in lower layers was relatively high, and some samples contained minor amount of inertinite, with a kerogen type index in the range of 23–87.2. Type II_1 kerogen was the dominant component in the lower layers. Based on a comparison of results, the type of OM in the upper layers is the best for petroleum generation, and then OM in evaporite layers; the lower layers are last, in terms of source rock potential.

4.2.2. TOC

Results showed that the TOC content of the upper layers is highest, followed by the source rocks in the evaporite layers (Figure 5). The TOC in the upper layers was generally >2 wt% up to 5.32 wt%, with an average of 3.39 wt%, while the TOC in the lower layers was mostly below 1 wt%, but >0.5%, with several points >1 wt% near the bottom of the evaporite layers. The variation in TOC content was larger in the evaporite layers. For most samples from the mudstones interbedded in the evaporite layers, the TOC was higher than 1 wt%, indicating good OM abundance.

4.2.3. Chloroform Extracts of Source Rocks

Experimental results showed that the chloroform extract content of source rocks in the upper layers was highest, followed by the evaporite layers where the evaporite beds are widespread (Figure 5). The value of the chloroform extract content was above 0.1% in the evaporite layers, from 0.16% to 1.01%, which showed that OM is well developed in the mudstone of evaporite layers. The upper layers had high contents of chloroform extracts, from 0.26% to 2.85%, showing very good petroleum generation. However, the high chloroform extracts may be related to oil shale sheet. For the lower layers, the content of chloroform extracts was comparatively low compared to the upper and evaporite layers, from 0.1% to 0.40%, but all > 0.1%. All these data indicate that the Es_4 display potential for hydrocarbon generation.

The content of total hydrocarbons (saturated + aromatic hydrocarbons) increased with burial depth (Figure 5), while nonhydrocarbons decreased overall with burial depth. The content of total hydrocarbons in the upper layers was mainly 40–80 wt%, and 20–40 wt% for nonhydrocarbons. The content of total hydrocarbons in the evaporite layers was mainly 60–90 wt%, with nonhydrocarbons less than 20 wt%.

4.2.4. Hydrocarbon Generation Potential

For the Rock-Eval pyrolysis, with hydrocarbon generation potential ($S_1 + S_2$), <2 mg/g is regarded as poor, 2–6 mg/g is medium, and >6 mg/g is good [45,46]. $S_1 + S_2$ of the upper layers are mostly above 4 mg/g, with about 70% >6 mg/g, and a maximum of 35.36 mg/g. The average was 13.34 mg/g in our research area. The value of hydrocarbon generation potential in the evaporite layers showed a wide variation of 1.33–13.54 mg/g, mostly above 4 mg/g, with an average of 6.62 mg/g. $S_1 + S_2$ in the lower layers was mostly below 2 mg/g, with an average of 1.59 mg/g and a maximum of 3.39 mg/g.

4.2.5. Carbon Isotopes

The analysis of carbon isotopes for different group components of extracts from Es_4 in wells FS1, FS2, and F8 in the Minfeng Sag showed that carbon isotope values are heavy overall (Figure 6a–c). The value of $\delta^{13}C$ of alkanes was $>-27.4‰$, and values were bigger than $-25.3‰$ and $-25.6‰$ for aromatic hydrocarbons and nonhydrocarbons, respectively. The data in Figure 6a–c show that $\delta^{13}C$ in the lower and evaporite layers are heavier than those in the upper layers. Figure 6 shows that carbon isotope values elevated with the increasing burial depth. However, the variation with burial depth was modest in the evaporite layers and lower layers. This implies that the isotopes might be impacted by evaporite layers. Correlations between carbon isotopes and vitrinite reflectance may suggest an effect of maturity on carbon isotope values. The ^{12}C-^{12}C bond is weaker than ^{13}C-^{13}C and ^{12}C-^{13}C bonds, which results in a lower activation energy for chemical reactions. With increasing thermal evolution, ^{12}C-^{12}C bonds rupture first, enriching the residual OM in ^{13}C [47]. Thus, the carbon isotope values of evaporite and lower layers are heavier than those in the upper layers.

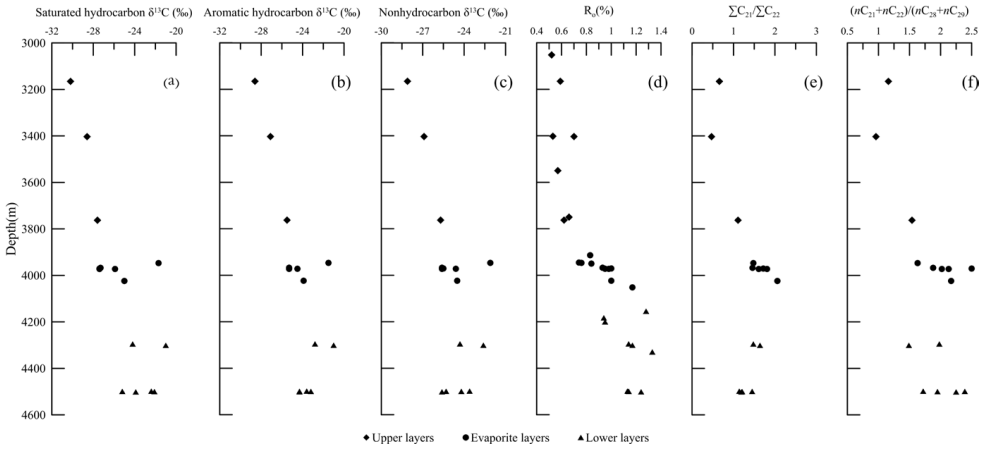


Figure 6. Carbon isotope ($\delta^{13}C$), Ro, $\sum C_{21}/\sum C_{22}$, and $(nC_{21} + nC_{22})/(nC_{28} + nC_{29})$ vs. burial depth of the evaporite-related source rocks in Es4 in the Dongying Depression. The samples were collected from wells F8, DF2, FS1, and FS2, which are located in the north belt of Dongying Depression. (**a**) Shows the $\delta^{13}C$ of saturated hydrocarbons changing with burial depth; (**b**) shows the $\delta^{13}C$ of aromatic hydrocarbons changing with burial depth; (**c**) shows the $\delta^{13}C$ of nonhydrocarbons changing with burial depth; (**d**) shows Ro changing with burial depth; (**e**) shows the ratios of $\sum C_{21}/\sum C_{22}$ changing with burial depth; (**f**) shows the ratios of $(nC_{21} + nC_{22})/(nC_{28} + nC_{29})$ changing with burial depth.

5. Discussion

5.1. Paleo-Environment

5.1.1. Paleoclimate

The final sediment composition depends primarily on its prevenance, which is modified by physical processes and associated geochemical alteration during transport from the source to the deposition area [48–52]. Rimmer [53] suggested that high amounts of Fe, Al, Ba, V, and Ni in lacustrine beds can indicate a high lake level, the desalination of the lake, and a humid environment. Conversely, high amounts of Na, Mg, Ca, Mn, and Sr indicate an arid climate [54,55]. The ratios of Fe/Mn, Sr/Ba, Sr/Ca, and Sr/Cu are commonly used to identify paleoclimates [53,56–59]. We adopted a multi-index method to infer the paleoclimate of Es_4 in the Dongying Depression, in order to reduce the uncertainty associated with various individual factors.

Experimental results showed that content of Sr firstly decreased and then increased in the lower layers, moving upward; however, Ba displayed the opposite trend (Figure 4). These trends suggest an arid climate during the early part of the deposition of the lower layers, becoming humid over time, and then drying once again [60]. This suggests an alternating dry–wet–dry cycle during the sedimentation of the lower layers. This observation is consistent with the results of Wang et al. [61]. The variation in elemental contents in the evaporite layers was greater; the content of Sr increased and decreased quickly, showing a sharp peak at the bottom of this section. Na and Mg both showed a large variation at the bottom, but become more stable in the upper section, suggesting relatively greater climate variation during the sedimentation of the latter units. Variations of Sr/Ba and Sr/Ca in the upper and evaporite layers were consistent, and greater than those in the lower layers. The Fe/Mn ratio was in contrast to the two former ratios. These data indicate that the climate of the evaporite-layer deposition was generally arid [53,56]. The contents of Mn and Ba increase in the upper layers, suggesting that the lake level had risen and deepened after the evaporites were deposited, and the lake had become less saline and the climate more humid. Similarly, the increased Fe and Al, decreased Mg and Sr, and increased Ca/Mg ratio suggest that the climate was more humid relative to the evaporite and lower layers.

5.1.2. Paleosalinity

The Sr/Ba ratio is sensitive to paleosalinity, because strontium sulfate is considerably more soluble than barium sulfate [60]. Mapila et al. [62] found that the Sr/Ca ratio of sedimentary rock can also be used to indicate paleosalinity, and shows a positive correlation consistent with Sr/Ba trends. A ratio of Sr/Ba < 1 indicates a terrestrial sedimentary environment (in which ratios between 0.6 and 1 indicate brackish water, whereas <0.6 indicates brackish-fresh water), whereas Sr/Ba > 1 indicates a saline lake environment [63–65]. Results (Figure 4) showed that the value of Sr/Ba in the lower layers decreased from > 1 to −0.1, and then increased to >1 again. This reflects the alternation of saline lacustrine facies (because of the evaporite beds in Ek) and brackish-fresh facies, transitioning to consistent saline lake facies. These data, combining the previous analysis of the paleoclimate, led us to conclude that the environment of the lower layer deposition was an intermittent salt lake-saline water environment. The values of Sr/Ba of the evaporite layers were mostly >1, suggesting mostly saline lacustrine facies with occasional brackish water. The Sr/Ba ratio of the upper layers was mostly 0.6-1 with a few outliers <0.6, indicating a brackish water environment for the upper layers.

5.1.3. Redox Environment

Sedimentary rocks can record the redox information of the depositional environment. The color of the mudstone in the lower layers of key well HK1 in the Central Uplift Belt is mainly dark red, purple and brown, with lesser grey mudstone (Figure 7), suggesting oxidizing conditions of deposition due to the presence of iron oxides in the mudstones. In addition, the pristane to phytane ratio (Pr/Ph) is commonly used to indicate the redox state of the dipositional environment [66–68]. Generally, Pr/Ph values above 1.0 indicate oxic conditions, while values below 1 indicate anoxic conditions [66]. But the Pr/Ph ratio is sensitive to maturity, and therefore caution should be taken when using it [69]. The Pr/Ph ratio increases before reaching the principal zone of oil formation, and then decreases. This phenomenon may lead to the redox conditions of deposition being misunderstood.

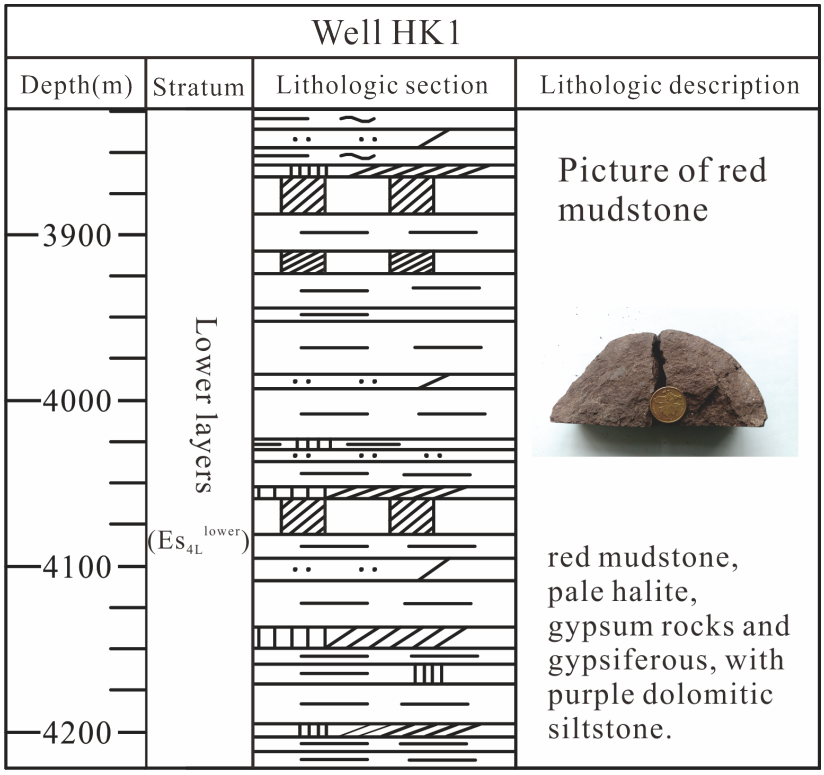


Figure 7. Lithologic section of the lower layers in well HK1.

We performed a statistical analysis of pristane and phytane in wells FS1, FS2, FS3, and F8 (Figure 8). All these wells are located in the Minfeng Sag. Experimental results indicated that low Pr/Ph (Pr/Ph < 0.7) and high phytane content appeared in the evaporite layers, while Ph/nC$_{18}$ showed high values (Ph/nC$_{18}$ > 2). These data suggest a strongly reducing, alkaline environment for evaporite layers. The Pr/Ph values were mostly <1 and decreased with the burial depth in the upper layers, which suggests a low-oxygen (anoxic) environment [70]. The Pr/Ph at 1.1 in the upper layers may have been caused by the source rock reaching the petroleum formation zone. However, phytane declines in the lower layers where Pr/Ph is 0.6–1.2, showing a slow increase. This reflects an oxygen variation (deficient-oxic) sedimentary environment in the lower layers. Furthermore, a ternary plot of Pr/Ph, Pr/nC$_{17}$, and Ph/nC$_{18}$ in Es$_4$ shows that the environmental conditions of OM deposition are consistent with the results of elemental analysis (Figure 9). For the northern steep slope of the Dongying Depression, source rocks in the lower layers are mostly distributed in Group III, with several at the border of Group III and II, which mainly indicates a fresh- to brackish-saline water sedimentary environment. Source rocks in the evaporite layers are mainly distributed in Group IV, indicating a salt lake environment. Additionally, source rocks in the upper layers are mostly distributed in Group III, with several in Group II, indicating a saline-subsaline to fresh-water sedimentary environment.

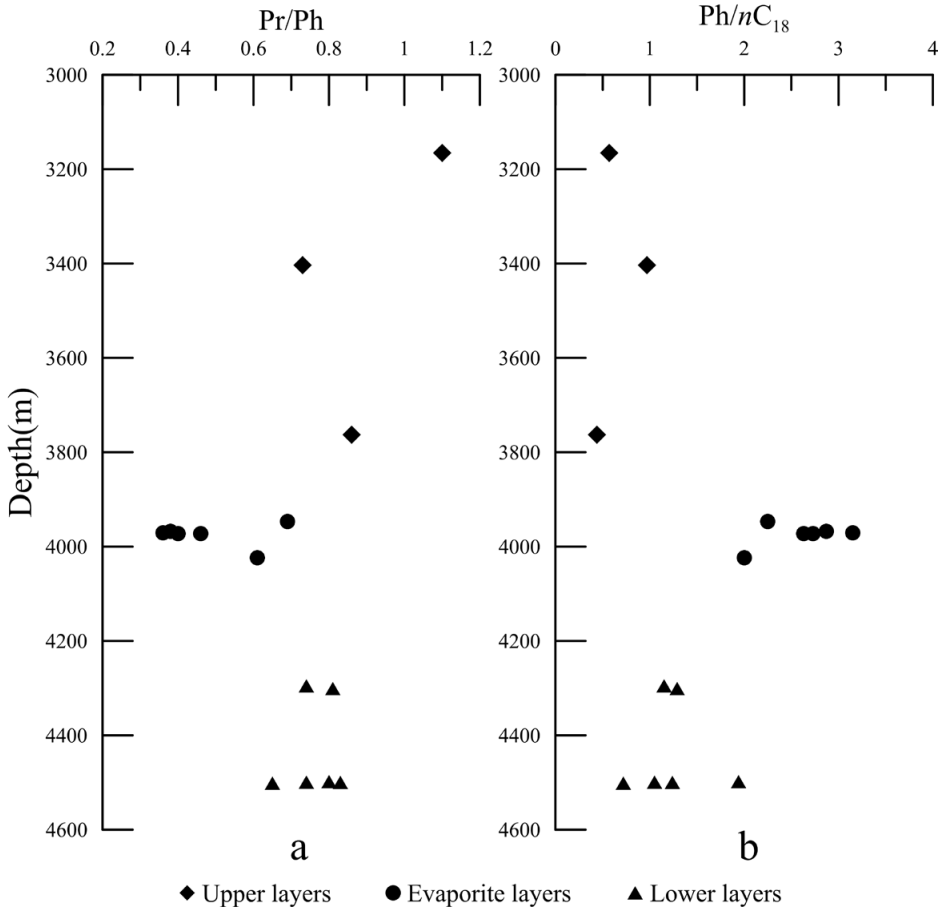


Figure 8. Burial depth vs. Pr/Ph (**a**) and Ph/nC18 (**b**) in the upper, evaporite, and lower layers. The samples were collected from wells FS1, FS2, FS3, and F8.

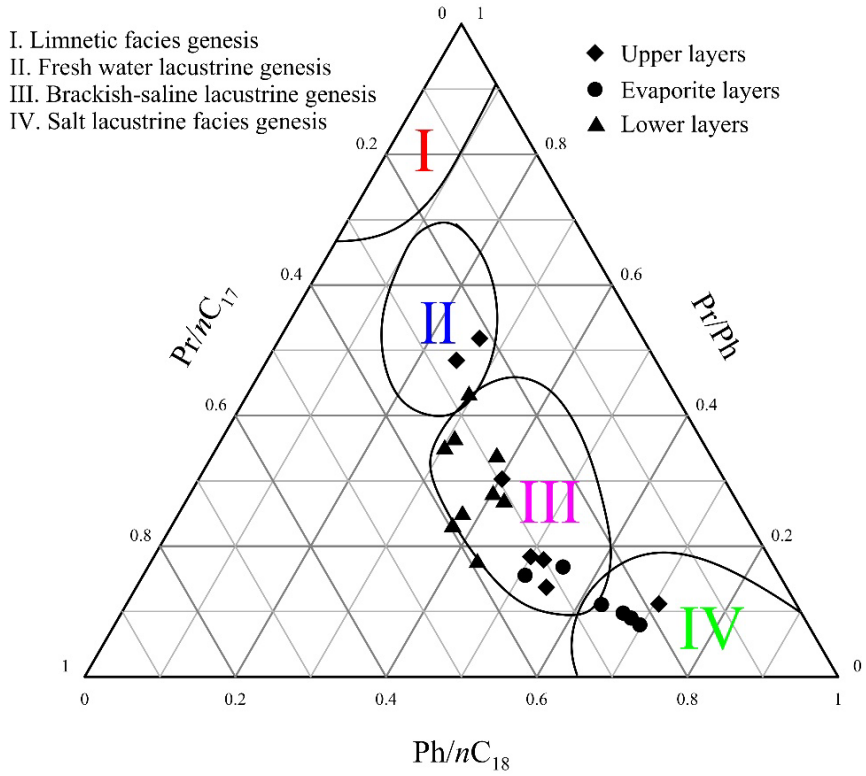


Figure 9. Pr/Ph, Pr/nC17, and Ph/nC_{18} of source rocks in Es_4 in the Dongying Depression. Board chart was revised after Wang et al. [33]. The samples were collected from wells F8, FS1, and FS2.

5.2. Organic Matter Richness

The accumulation and preservation of organic matter in sedimentary environments is controlled by primary productivity, sedimentary rate, settling time, redox conditions at the bottom, chemical composition, and the depth of the water. In this study, the formation and preservation of organic matter in a salt lake took place in a strong reducing environment (as described above). The high salinity in a salt lake makes it easy for a permanent halocline to form. The anoxic environment forms under bottom water characterized by high salinity, and the organic matter avoids decomposition via oxidation, resulting in the formation of high quality source rocks [25,37,42].

The studied samples were characterized by highly variable TOC contents, ranging from 0.35% to 5.32%. Peters and Cassa [69] presented standard guidelines for evaluating the organic richness, quality, and maturity of source rocks based on pyrolysis parameters in which a TOC value of 0.5 wt% was considered to be the base limit for an effective source rock. An effective source rock was defined as a rock which contains organic matter and is presently generating and/or expelling hydrocarbons to form commercial accumulations [71]. Based on the above standard, and in combination with previous studies [34], most source rocks (mudstone or shale) related to evaporites in this study were effective source rocks, which has been proved by drilling exploration. The TOC is low in the lower layers, and a previous researcher reported that the mudstone in the lower layers was still an effective source rock [44], but caution should be taken when exploring for petroleum.

The TOC difference between the lower, evaporite, and upper layers is firstly due to the sedimentary environment. The enrichment of nutrients in brackish to fresh water, such as nitrogen and phosphorus compounds, can promote the production of plankton and algae, resulting in higher productivity [25,72,73]. This may be the reason for the high TOC in the upper layers. Yuan et al. [23], Chen et al. [74], and Ma et al. [75] reported that deep basins in mountainous terrains (like the Dongying Depression) are suitable for the formation of a halocline, causing salinity stratification and promoting the formation of a reducing horizon

in deeper water (identified by Pr/Ph). Former discussions showed that the upper layers were formed in this latter regime, where OM preservation is favored. The variation in TOC content is larger in the gypsum-salt layers. For most samples, the TOC was higher than 1%, showing a good OM abundance, and was better than the source rock in Holocene-Pleistocene salt flat sabkha (playa), W-Texas-New Mexico [76]. Moreover, the presence of gammacerane suggests water, but also hypersalinity column stratification [77,78], and the TOC content of the evaporite layers was positively associated with gammacerane content (Figure 5), which is related to water salinity and stratification. Brine stratification inhibited the free circulation of oxygen in the lake bottom, enhancing the preservation of organic matter [77]. This suggests that the OM content is related to the salinity of the lake. The sedimentary environment of the lower layers is an intermittent salt lake–saline water environment, and the paleo-productivity of the OM is lower than in the upper and evaporite layers. The oxidation state is suboptimal for the preservation of OM. All these factors led to the lower OM content of source rocks in lower layers compared to the other layers.

According to the above analysis, the environment of the evaporite layer deposition was a reducing salt lake environment, and a saline lacustrine sedimentary environment was present for the upper layers. The depositional environment was suitable for OM preservation. The values of $S_1 + S_2$ (hydrocarbon generation potential) show a positive correlation with TOC. This also indicates that reducing the sedimentary environment with saline water is favorable to the enrichment and preservation of OM. These results show that source rocks in the evaporite and upper layers have better hydrocarbon generation potential than in the lower layers. Several samples showed high extract contents because of oil shale-bearing in the upper layers.

For the source rocks of E_{s4} in the Dongying Depression, the effective and good source rocks were generally those with TOC > 0.5%, hydrocarbon generation potential > 2mg/g, and chlolroform extract content > 0.1%, according to a previous study [32,44] and the exploration of the Shengli Oilfield Company. Based on this, and considering the reliability of the conclusion, using the limit of TOC >1% in present study, the results (in Figure 5) showed that most samples in the upper and evaporite layers were effective and good source rocks for petroleum generation, while those in the lower layers might be potential source rocks.

5.3. Thermal Evolution of Source Rocks

For source rocks, the vitrinite reflectance (R_o), carbon isotopes, production index, T_{max}, and hydrocarbon content change with thermal maturity. We addressed R_o, T_{max}, production index, carbon isotopes, and hydrocarbon content to assess thermal maturity.

5.3.1. Vitrinite Reflectance

The studied samples were from wells DF2, FS2, and F8, which are located in the northern steep-slope belt of the Dongying Depression. The analysis results of vitrinite reflectance (R_o) data of E_{S4} source rocks (Figure 6d) showed that R_o increased with the burial depth. The rate at which R_o increased with the burial depth in the upper and evaporite layers was greater than in the lower layers. The rate slowed just below the bottom of the evaporite layers, likely reflecting the high conductivity of evaporite beds, which was 2–5 times greater compared to shale [21,29]. The thermal conductivity of shale above the evaporite beds was lower, allowing heat accumulation in the upper evaporite layers and the above strata. Because the evaporite layers contain three sets of evaporite beds and the source rocks are interbedded with them, like in the sandwich model, this leads to heat being accumulated in these source rocks (shale and mudstones) in the evaporite layers. Thus, the R_o of the evaporite layers and the strata above was significantly increased, and showed a high Ro gradient. A similar phenomenon was also found in other evaporite-bearing basins, such as the Gulf of Mexico basin [29] and the Tarim Basin [30]. It has been proved that the evaporite layers can impact on the geothermal temperature profile and

result in an effect on the thermal maturity of source rocks [29,30]. Usually, there is a quick rise of Ro near the evaporite layers and Ro increases slowly below salt beds.

Figure 10 shows the difference in Ro between the upper layers and evaporite-free areas at similar burial depths in the Dongying Depression. All the samples in the present study had similar burial and geothermal histories. Based on contrasting analyses of R_o of the strata above the evaporite layers and the area without evaporites at similar burial depths (Figure 10), results showed that the R_o of the upper layers were mostly greater than 0.6%, while the R_o of the area without evaporites were lower (0.4–0.5%). This also suggests that the high conductivities of evaporite beds increased the thermal flow in the above strata, increasing the thermal evolution of the OM in the upper layers. This process led to a higher R_o in the upper layers, compared to the areas without evaporite beds at the same burial depth. This was consistent with the distribution of R_o in Figure 10. These data indicate that evaporites can promote the thermal evolution of OM of source rocks in the upper layers near the evaporite layers.

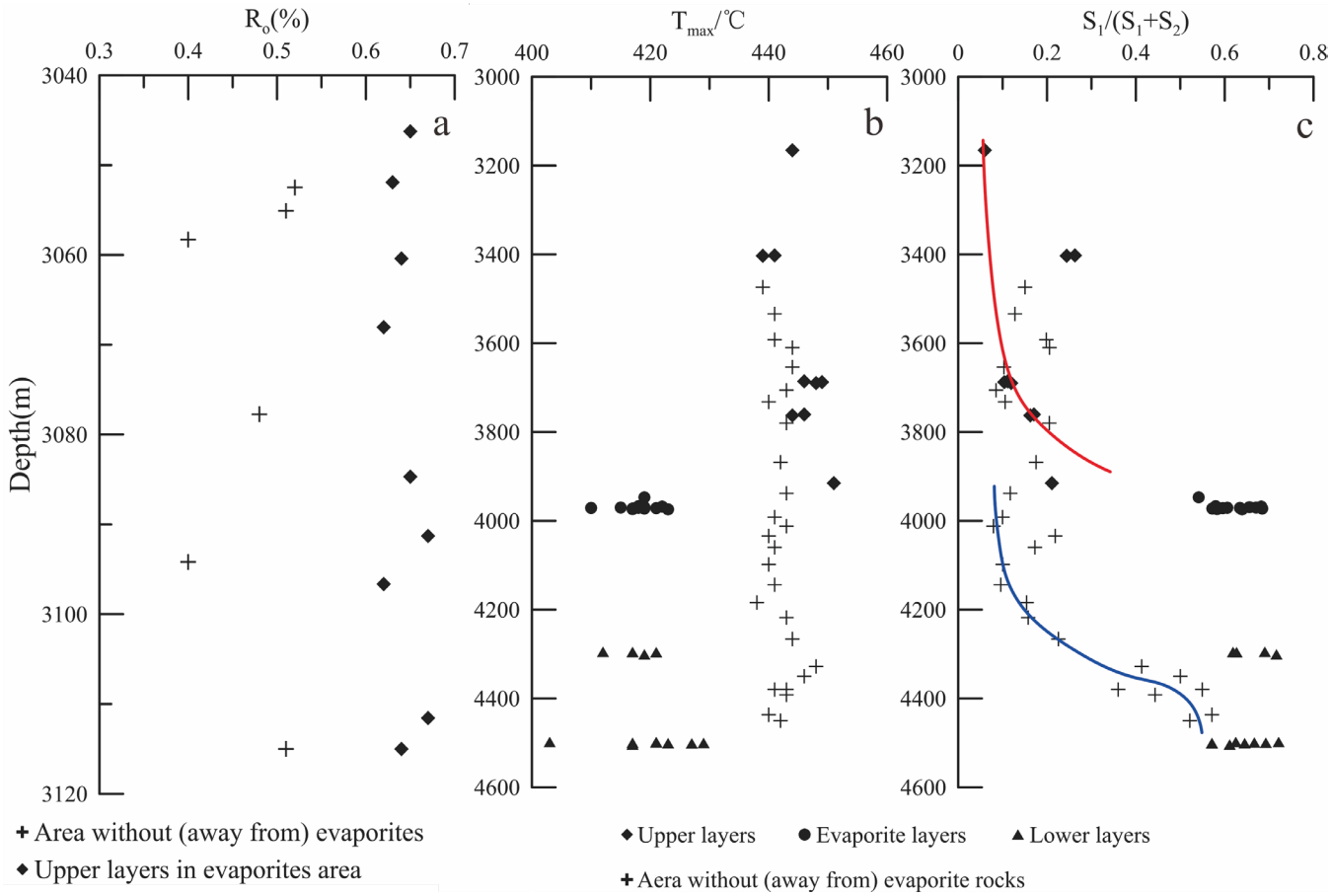


Figure 10. (**a**) Comparison of Ro in the upper layers and evaporite-free areas at similar burial depths. The samples of the upper layers were collected from well DF5, and the samples of evaporite-free area were collected from wells T762, N35, and DF2. (**b**) T_{max} vs. burial depth. (**c**) $S_1/(S_1 + S_2)$ vs. burial depth. The red trend curve in (**c**) shows the change in $S_1/(S_1 + S_2)$ with burial depth in the evaporite-bearing area; the blue one shows those in the evaporite-free area. The samples of evaporite bearing area were collected from wells FS1, F8, and FS2, and the samples of evaporite-free area were collected from well XLS1.

5.3.2. T_{max}

The T_{max} of source rocks in the upper layers (wells FS1 and F8), evaporite, and lower layers (well FS2) and the samples of areas far from evaporite beds (well XLS1) was compared (Figure 10b). The results showed that the T_{max} of samples from the upper layers

was about 440–450°C, whereas that of the evaporite and lower layers was about 420 °C. The T_{max} of the samples far from evaporite beds increased slightly with burial depth, but fluctuated between ~440 and 450 °C. The T_{max} in the lower layers was obviously lower than those of the area away from the evaporite beds, while the upper layers did not show this phenomenon. The low T_{max} values in the evaporite and lower layers (Figure 10) might have been affected by the accumulation of hydrocarbons [38,79], as some shale oil (soluble organic matter) was found in the lower layers according to the drilling data from Shengli Oilfield Company. The T_{max} values in the upper layers increased near to evaporite beds. This also indicates a high thermal maturity of the source rock in the upper layers, near the evaporites. Although the low T_{max} values might be caused by some accumulated hydrocarbons, the increasing trend of T_{max} is similar to the variation in R_o in the upper layer (Figure 6d). Because the R_o is not affected by accumulated hydrocarbons, we can infer that the variation trend of T_{max} is similar to R_o. Therefore, the low T_{max} in the evaporite and lower layers could be caused by two reasons; one is the accumulated hydrocarbons, and the other is the geothermal temperature being affected by the evaporite beds. Which one is the main factor will be clarified in future study.

In any case, the variations in R_o and T_{max} showed that evaporite beds can slow down the evolution of OM in lower layers because of the high thermal conductivities of salt rock beds. Therefore, the diagenetic evolution was restrained and the evolution of source rocks differed relative to comparable levels of those in the area without evaporite beds. Thus, the burial depth of source rocks for reaching high maturity was deepened, and the oil generation window is widened. Moreover, abnormally high pore pressures in the evaporite layers and underlying strata result from the strong plasticity and compactness of gypsum-salt rocks, restraining the maturation of OM and the cracking of hydrocarbons of the source rocks in lower layers [25,80,81]. Physical sealing and pressure sealing mechanisms are the important factors that result in the strata of overpressure sealing [82], and the pressure coefficients in the evaporite-bearing area were a little higher than those of the evaporite-free area. For example, in the layers where evaporite beds are widespread, in well HK1, 3351–3825 m depth, the pore pressure coefficient reached up to 1.5–1.91, showing high overpressure. And, in the strata containing evaporites in well TS1, at 3580–4000 m depth, the pore pressure coefficients reached medium-high overpressure (about 1.6). Thus, the presence of evaporites affected not only the heat transmission, but also the pore pressure, which resulted in R_o and T_{max} showing variation, as described above.

5.3.3. Production Index ($S_1/(S_1 + S_2)$)

The production index (PI), the ratio of $S_1/(S_1 + S_2)$, can be used to indicate the maturity of OM. Usually, a high PI means that the source rock contains more soluble hydrocarbons, which are the expelled petroleum of the source rock, and indicates a good hydrocarbon generation potential of the source rock [72]. The PI of source rocks in the upper layers (wells FS1 and F8), evaporite, and lower layers (well FS2) and the area without salt rock beds (well XLS1) (Figure 10c) were analyzed. The results showed good correlations between the variation trend in $S_1/(S_1 + S_2)$ and R_o (Figure 6d). In addition, a comparison between curves revealed that the burial depth for source rocks in the upper layers to become mature was shallower relative to the samples from the area without evaporite beds. This illustrates that evaporites can reduce the hydrocarbon generation threshold (burial depth) and allow the oil generation window to appear earlier. The PI of source rocks in the evaporite and lower layers was much greater than that from the area without evaporites at the same burial depth. This might indicate a good hydrocarbon generation potential for source rocks in the evaporite and lower layers. However, the high ratio of $S_1/(S_1 + S_2)$ in the lower layers may be caused by the accumulation of hydrocarbons, as mentioned above. Care should be taken to assess the source rocks in the evaporite and lower layers.

5.3.4. Isotopes, $(nC_{21} + nC_{22})/(nC_{28} + nC_{29})$, and $\sum C_{21}/\sum C_{22}$ Change with Maturity

The carbon isotopes of saturated, aromatic hydrocarbon and nonhydrocarbon groups showed the same trend as vitrinite reflectance, increasing with burial depth. The value of the carbon isotope increased with burial depth in the upper layers, and the rate of increasing became quicker near to the evaporites beds. But there was no obvious increase for the carbon isotope in the evaporite and lower layers. This also indicates that the source rocks in the evaporite and lower layers had a slower thermal evolution rate than in the upper layers.

The data of rock chloroform extracts and saturated hydrocarbon gas chromatography parameters were analyzed statistically, as shown in Figure 6e,f. Results showed that $(nC_{21} + nC_{22})/(nC_{28} + nC_{29})$ and $\sum C_{21}/\sum C_{22}$ increased with burial depth and were correlated, reflecting the increasing maturity of the source rock. As seen in Figure 6e,f, the two parameters increased with the burial depth from the upper layers to the evaporite layers, while those of some samples in the lower layers were mainly unchanged or lowered slightly. Once again, this suggests that the evaporite rocks could restrain the evolution of OM in the lower layers.

6. Conclusions

In this study, we presented the results of a comparative study of evaporite-related source rocks of the fourth member of the Shahejie Formation in the Dongying Depression, through analyses of their characteristics in terms of the total content of organic matter, the kerogen type, and the quality and maturity level, together with the analysis of their hydrocarbon generation potential. Based on our results and analyses, the following conclusions can be reached.

(1) The sedimentary environment changed from the lower layers to the upper layers and resulted in the differences in evaporite-related source rocks in Es_4 in the Dongying Depression. The lower layers were deposited in an intermittent saline lake environment in a relatively dry climate. The evaporite layers were formed in a highly saline lake environment in an arid climate, whereas the upper layers were formed in a brackish-saline to fresh-water environment in a humid climate.

(2) The content of TOC, hydrocarbon generation potential, and chloroform extracts of most studied samples indicated a good potential for hydrocarbon generation. The geochemical parameters showed that the source rocks for petroleum generation in the upper layers were the best, the evaporite layers were medium, and the lower layers were poor in comparison.

(3) Thermal maturity parameters (including R_o, T_{max}, PI and chloroform extracts) and carbon isotopes showed that the thermal evolution process of OM in the upper layers was faster than in the evaporite-free areas, while the thermal evolution of OM in the lower layers was slower than elsewhere. The high thermal conductivity of anhydrite and halite may have accelerated the thermal evolution of source rocks in upper layers near the evaporite beds and allowed hydrocarbon generation at shallower burial depths than those in areas without evaporites. This resulted in the earlier appearance of the petroleum generation window, compared to evaporite-free areas. Meanwhile, the thermal evolution of OM in lower layers was restrained, and consequently the hydrocarbon generation window was widened, which implies a potential for petroleum exploration in deep strata under the evaporites sequence. However, because the T_{max} and $S_1/(S_1 + S_2)$ in the evaporite and lower layers were affected by accumulated hydrocarbons, we should be careful to use these parameters to assess the source rocks in the lower layers, and detailed work need to be carried out in future studies.

Author Contributions: Conceptualization, Y.C.; Methodology, Y.C., Y.H. and Y.Q.; Validation, Y.H. and M.W.; Investigation, Y.Q.; Resources, Y.C., Y.H., P.Z., Y.Q. and X.Z. (Xuejun Zhang); Writing—original draft, Y.C., Y.H. and M.W.; writing—review and editing, Y.C., P.Z., M.W. and X.Z. (Xuelei Zhu); Supervision, Y.C.; Funding acquisition, Y.C. All authors have read and agreed to the published version of the manuscript.

Funding: This research was funded by the National Natural Science Foundation of China [No. 41172111, U1762108 and 41873070], the Shandong Provincial Natural Science Foundation [No. ZR2021QD012], and the Key Research Projects of Shandong Province [No. 2017CXGC1608 and 2017CXGC1602].

Data Availability Statement: Data is unavailable due to privacy.

Acknowledgments: We appreciate the Institute of Geological Sciences of Shengli Oilfield Company, SINOPEC, for offering some data and samples. We would like to thank Matthew Steele-MacInnis for his constructive suggestions.

Conflicts of Interest: The authors declare no conflict of interest.

References

1. Hudec, M.R.; Jackson, M.P.A. Advance of allochthonous salt sheets in passive margins and orogens. *AAPG Bull.* **2006**, *90*, 1535–1564. [CrossRef]
2. Hudec, M.R.; Jackson, M.P.A. Terra infirma: Understanding salt tectonics. *Earth Sci. Rev.* **2007**, *82*, 1–28. [CrossRef]
3. Warren, J.K. *Evaporites: Sediments, Resources, and Hydrocarbons*; Springer: Berlin/Heidelberg, Germany, 2006; p. 1035.
4. Warren, J.K.; Cheung, A.; Cartwright, I. Organic geochemical, isotopic, and seismic indicators of fluid flow in pressurized growth anticlines and mud volcanoes in modern deep-water slope and rise sediments of offshore Brunei Darussalam; implications for hydrocarbon exploration in other mud- and salt-diapir provinces (in Shale tectonics). *AAPG Mem.* **2010**, *93*, 163–196.
5. Keen, C.E. Salt diapirs and thermal maturity: Scotian Basin. *Bull. Can. Petrol. Geol.* **1983**, *31*, 101–108.
6. Hills, J.M. Sedimentation, tectonism, and hydrocarbon generation in Delaware Basin, West Texas and Southeastern New Mexico. *AAPG Bull.* **1984**, *68*, 250–267.
7. Edgell, H.S. Salt tectonics in the Persian Gulf Basin. In *Geological Society of London Special Publication, 2ne ed.*; Alsop, G.I., Blundell, D.J., Davidson, I., Eds.; Geological Society of London Special Publication: London, UK, 1996; Volume 100, pp. 129–151.
8. Konyuhov, A.I.; Malek, B. The Persian Gulf Basin: Geological history, sedimentary formations, and petroleum potential. *Lithol. Miner. Resour.* **2006**, *41*, 344–361. [CrossRef]
9. Peryt, T.M.; Geluk, M.C.; Mathiesen, A.; Paul, J.; Smith, K. Zechstein. In *Petroleum Geological Atlas of the Southern Permian Basin Area*, 2nd ed.; Doornenbal, J.C., Stevenson, A.G., Eds.; EAGE Publications: Houten, The Netherlands, 2010; pp. 123–147.
10. Rowan, M.G.; Jackson, M.P.A.; Trudgill, B.D. Salt-related fault families and fault welds in the Northern Gulf of Mexico. *AAPG Bull.* **1999**, *83*, 1454–1484.
11. Stover, S.C.; Weimer, P.; Ge, S.M. The effective of allochthonous salt evolution and overpressure development on source rock thermal maturation: A two-dimensional transient study in the northern Gulf of Mexico Basin. *Petrol. Geosci.* **2001**, *7*, 281–290. [CrossRef]
12. Hadad, Y.T.; Abdullah, W.H. Hydrocarbon source rock generative potential of the Sudanese Red Sea basin. *Mar. Petrol. Geol.* **2000**, *65*, 269–289. [CrossRef]
13. Davison, I.; Dailly, P. Salt tectonics in the Cap Boujdour Area, Aaiun Basin, NW Africa. *Mar. Petrol. Geol.* **2010**, *27*, 2435–2441. [CrossRef]
14. Stovba, S.M.; Stephenson, R.A. Style and timing of salt tectonics in the Dniepr-Donets Basin (Ukraine): Implications for triggering and driving mechanisms of salt movement in sedimentary basins. *Mar. Petrol. Geol.* **2003**, *19*, 116–1189. [CrossRef]
15. Schubel, K.A.; Lowenstein, T.K. Criteria for the Recognition of Shallow-Perennial-Saline-Lake Halites Based on Recent Sediments From the Qaidam Basin, Western China. *J. Sediment. Res.* **1997**, *67*, 74–87.
16. Jin, Q.; Zha, M. Co-sedimentation of Tertiary evaporites and oil source rocks in the western Qaidam basin. *Sci. Geol. Sin.* **2000**, *35*, 465–473, (In Chinese with English Abstract).
17. Hanson, A.D.; Ritts, B.D.; Zinniker, D. Upper Oligocene lacustrine source rocks and petroleum systems of the northern Qaidam Basin, north-west China. *AAPG Bull.* **2001**, *85*, 601–620.
18. Wan, G.M.; Tang, L.J.; Jin, W.Z. Function of salt rock in Kuqa depression. *J. Southwest. Petrol. Univ. Sci. Technol. Ed.* **2008**, *30*, 14–17, (In Chinese with English abstract).
19. Yu, Y.X.; Tang, L.J.; Yang, W.J.; Huang, T.Z.; Qiu, N.S.; Li, W.G. Salt structures and hydrocarbon accumulations in the Tarim Basin, northwest China. *AAPG Bull.* **2014**, *98*, 135–159. [CrossRef]
20. Du, H.F.; Yu, X.H.; Chen, F.L. Sedimentary characteristics of salt rocks and their petroleum geologic significance of the Member 3 of Shahejie Formation of Paleogene in Dongpu Depression, Henan Province. *J. Palaeogeogr.* **2008**, *10*, 53–62.
21. Liu, J.D.; Jiang, Y.L.; Tan, Y.M. Relationship between gypsum-salt rock and oil-gas in Dongpu depression of Bohai Gulf Basin. *Acta Sedimentol. Sin.* **2014**, *32*, 126–137, (In Chinese with English Abstract).
22. Ma, P.; Lin, C.; Dong, C.; Ren, L.; Jahren, J.; Hellevang, H.; Lin, J. Effect of faulting on diagenetic processes in the silicate-sulfate-carbonate system: A case study from the Bonan Sag of Jiyang Depression, Bohai Bay Basin. *Mar. Petrol. Geol.* **2023**, *147*, 105985. [CrossRef]

23. Yuan, J.; Qin, K. Characteristics of evaporite generated in deep water of sha-4 member in Dongying depression. *J. Univ. Pet.* **2001**, *25*, 9–11, (In Chinese with English Abstract).
24. Xu, L.; Cao, Y.; Wang, Y.; Huang, L. Genetic model of salt-gypsum rock of Paleogene in Dongying depression and its relationship with hydrocarbon reservoir. *J. Univ. Pet.* **2008**, *32*, 30–35, (In Chinese with English Abstract).
25. Kirkland, D.W.; Evans, R. Source-rock potential of evaporitic environment. *AAPG. Bull.* **1981**, *65*, 181–190.
26. Busson, G. Relationship between different types of evaporitic deposits, and the occurrence of organic-rich layers (potential source-rocks). *Carbonates Evaporites* **1991**, *6*, 177–191. [CrossRef]
27. Sellig, F.; Wallick, G.C. Temperature distribution in salt domes and surrounding sediments. *Geophysics* **1966**, *31*, 346–361. [CrossRef]
28. O'Brien, J.J.; Lerche, I. The influence of salt domes on paleotemperature distributions. *Geophysics* **1984**, *49*, 2032–2043. [CrossRef]
29. Mello, U.T.; Karner, G.D.; Anderson, R.N. Role of salt in restraining the maturation of subsalt source rocks. *Mar. Petrol. Geol.* **1995**, *12*, 697–716. [CrossRef]
30. Zhuo, Q.G.; Meng, F.W.; Zhao, M.J.; Li, Y.; Lu, X.S.; Ni, P. The salt chimney effect: Delay of thermal evolution of deep hydrocarbon source rocks due to high thermal conductivity of evaporites. *Geofluids* **2016**, *16*, 440–451. [CrossRef]
31. Seewald, J.S. Organic-inorganic interactions in petroleum-producing sedimentary basins. *Nature* **2003**, *20*, 326–332. [CrossRef]
32. Zhu, G.Y.; Jin, Q.; Wang, R. Identification methods for efficient source rocks. *J. Univ. Pet.* **2003**, *27*, 6–10, (In Chinese with English Abstract).
33. Wang, R. Geochemical characteristics and source of light oil in the deep Es4 lower layers underlying salt in the northern Dongying depression. *Nat. Gas Geosci.* **2009**, *20*, 278–281, (In Chinese with English Abstract).
34. Guo, X.W.; Liu, K.Y.; He, S.; Song, G.Q.; Wang, Y.S.; Hao, X.F.; Wang, B.J. Petroleum generation and charge history of the northern Dongying Depression, Bohai Bay Basin, China: Insight from integrated fluid inclusion analysis and basin modeling. *Mar. Petrol. Geol.* **2012**, *32*, 21–35. [CrossRef]
35. Yuan, G.H.; Gluyas, J.; Cao, Y.C.; Oxtoby, N.H.; Jia, Z.Z.; Wang, Y.Z.; Xi, K.L.; Li, X.Y. Diagenesis and reservoir quality evolution of the Eocene sandstones in the northern Dongying Depression, Bohai Bay Basin, East China. *Mar. Petrol. Geol.* **2015**, *62*, 77–89. [CrossRef]
36. Zhou, Z.Z. The Evolution of Geotemperature-Geopressure Fields and Hydrocarbon Accumulation in Deep Reservoirs Underlying Gypsum-Salt Strata in Dongying Depression. Ph.D. Thesis, China University of Petroleum (East China), Beijing, China, 2011. (In Chinese with English Abstract).
37. Chen, Z.H.; Zhang, J.Q.; Wang, L.; Zha, M. Geochemistry of Evaporites in Lacustrine Basin, Dongying Depression, Bohai Bay Basin, China. *J. Pet. Environ. Biotechnol.* **2013**, *4*, 5.
38. Zhang, Z.L.; Wu, L.Y.; Shu, N.Z. Cause analysis of abnormal T_{max} values on Rock-Eval pyrolysis. *Petrol. Explor. Dev.* **2006**, *33*, 72–75.
39. Wang, M.; Chen, Y.; Song, G.; Steele-MacInnis, M.; Liu, Q.; Wang, X.; Zhang, X.; Zhao, Z.; Liu, W.; Zhang, H.; et al. Formation of bedding-parallel, fibrous calcite veins in laminated source rocks of the Eocene Dongying Depression: A growth model based on petrographic observations. *Int. J. Coal Geol.* **2018**, *200*, 18–35. [CrossRef]
40. Wang, M.; Chen, Y.; Bain, W.M.; Song, G.; Liu, K.; Zhou, Z.; Steele-MacInnis, M. Direct evidence for fluid overpressure during hydrocarbon generation and expulsion from organic-rich shales. *Geology* **2020**, *48*, 374–378. [CrossRef]
41. Huang, B.; Tian, H.; Li, X.; Wang, Z.; Xiao, X. Geochemistry, origin and accumulation of natural gases in the deepwater area of the Qiongdongnan Basin, South China Sea. *Mar. Petrol. Geol.* **2016**, *72*, 254–267. [CrossRef]
42. Tissot, B.P.; Welte, D.H. *Petroleum Formation and Occurrence*, 3rd ed.; Second revised and enlarged edition; Springer: Berlin/Heidelberg, Germany, 1984.
43. Li, T.M.; Lu, S.F. A numerical kerogen type index. *J. Petrol. Geol.* **1990**, *13*, 87–92.
44. Gao, Y. Characteristics and distribution of salt lake source rocks from lower submemeber of 4th member of Shahejie formation, north Dongying depression. *Pet. Geol. Recovery Effic.* **2014**, *21*, 10–15, (In Chinese with English Abstract).
45. Espitalié, J.; LaPorte, J.L.; Madec, M.; Marquis, F.; LePlat, P.; Paulet, J.; Boutefeu, A. Rapid method for source rocks characterization and for determination of petroleum potential and degree of evolution. *Oil Gas Sci. Technol.* **1977**, *32*, 23–42.
46. Yang, R.; Cao, J.; Hu, G.; Fu, X. Organic geochemistry and petrology of Lower Cretaceous black shales in the Qiangtang Basin, Tibet: Implications for hydrocarbon potential. *Org. Geochem.* **2015**, *86*, 55–70. [CrossRef]
47. Arneth, J.D.; Matzigkeit, U. Laboratory-simulated thermal maturation of different types of sediments from the Williston Basin, North America-effects on the production rates, the isotopic and organo-geochemical composition of various pyrolysis products. *Chem. Geolo. Isot. Geosci. Sect.* **1986**, *58*, 339–360. [CrossRef]
48. Nesbitt, H.W.; Young, G.M. Early Proterozoic climates and plate motions inferred from major element chemistry of lutites. *Nature* **1982**, *299*, 715–717. [CrossRef]
49. Francois, R. A study on the regulation of the concentrations of some trace elements (Rb, Sr, Zn, Pb, Cu, V, Cr, Ni, Mn and Mo) in Saanich Inlet sediments, British Columbia, Canada. *Mar. Geol.* **1988**, *83*, 285–308. [CrossRef]
50. Cullers, R.L. The controls on the major and trace element evolution of shales, siltstones and sandstones of Ordovician to Tertiary age in the Wet Mountainregion, Colorado, USA. *Chem. Geol.* **1995**, *123*, 107–131. [CrossRef]
51. Cullers, R.L. The geochemistry of shales, siltstones and sandstones of Pennsylvanian-Permian age, Colorado, USA: Implications for provenance andmetamorphic studies. *Lithos* **2000**, *51*, 181–203. [CrossRef]
52. Cullers, R.L. Implications of elemental concentrations for provenance, redoxconditions, and metamorphic studies of shales and limestones near Pueblo, CO, USA. *Chem. Geol.* **2002**, *191*, 305–327. [CrossRef]
53. Rimmer, S.M. Geochemical paleoredox indicators in Devonian-Mississippian black shales, Central Appalachian Basin (USA). *Chem. Geol.* **2004**, *206*, 373–391. [CrossRef]

54. Calvert, S.E.; Pedersen, T.F. Geochemistry of Recent oxic and anoxic marine sediments: Implications for the geological record. *Mar. Geol.* **1993**, *113*, 67–88. [CrossRef]
55. Qiu, H.; Sun, W.; Yang, Z. Geochemical Characteristics of the Oma Section in the Tibetan Gyirong Basin and Its Implications on Environment Change. *Earth Sci. J. China Univ. Geosci.* **2010**, *35*, 789–802, (In Chinese with English Abstract).
56. Smith, A.J.; Donovan, J.J.; Ito, E.; Engstrom, D.R.; Panek, V.A. Climate-driven hydrologic transients in lake sediment records: Multiproxy record of mid-Holocene drought. *Quatern. Sci. Rev.* **2002**, *21*, 625–646. [CrossRef]
57. Li, C.; Chen, K. Evolutional characteristics and their Paleoclimate significance of elements in the Qianjiang formation, Qianjiang depression. *Petrol. Geol. Eng.* **2007**, *21*, 18–21, (In Chinese with English Abstract).
58. Kong, F.; Yang, R.; Wei, H.; Wen, X.; Han, X.; Gao, J. Geochemistry of trace elements of the Quaternary sediments of Yaoshang formation in Weining county, Guizhou province and its paleoenviromental implications. *Mar. Geol. Quatern. Geol.* **2011**, *31*, 117–125. [CrossRef]
59. Fathy, D.; Abart, R.; Wagreich, M.; Gier, S.; Ahmed, M.S.; Sami, M. Late campanian climatic-continental weathering assessment and its influence on source rocks deposition in southern Tethys, Egypt. *Minerals* **2023**, *13*, 160. [CrossRef]
60. Liu, G.; Zhou, D. Application of microelements analysis in identifying sedimentary environment—Taking Qianjiang Formation in the Jianghan Basin as an example. *Petrol. Geol. Exp.* **2007**, *29*, 307–314, (In Chinese with English Abstract).
61. Wang, J.; Cao, Y.; Liu, H.; Gao, Y. Characteristics of Sedimentary Environment and Filling Model of the Lower Submember of the Fourth Member of Shahejie Formation, Dongying Depression. *Acta Sedimentol. Sin.* **2012**, *30*, 74–83, (In Chinese with English abstract).
62. Mapila, H.P.; Ringrose, S.; Mackay, A.W.; Downey, W.S.; Modisi, M.; Coetzee, S.H.; Tiercelin, J.-J.; Kampunzu, A.B.; Vanderpost, C. Use of the geochemical and biological sedimentary record in establishing palaeo-environments and climate change in the Lake Ngami basin, NW Botswana. *Quatern. Int.* **2006**, *148*, 51–54. [CrossRef]
63. Janz, H.; Vennemann, T.W. Isotopic composition (O, C, Sr, and Nd) and trace element ratios (Sr/Ca, Mg/Ca) of Miocene marine and brackish ostracods from North Alpine Foreland deposits (Germany and Austria) as indicators for palaeoclimate. *Palaeogeogr. Palaeoclimatol. Palaeoecol.* **2005**, *225*, 216–247. [CrossRef]
64. Medina-Elizalde, M.; Lea, D.W.; Fantle, M.S. Implications of seawater Mg/Ca variability for Plio-Pleistocene tropical climate reconstruction. *Earth Planet. Sci. Lett.* **2008**, *269*, 585–595. [CrossRef]
65. Fan, Y.; Qu, H.; Wang, H.; Yang, X.; Feng, Y. The application of trace elements analysis to identifying sedimentary media Environment: A case study of Late Triassic strata in the middle part of western Ordos Basin. *Geol. China* **2012**, *39*, 382–389, (In Chinese with English Abstract).
66. Didyk, B.M.; Simoneit, B.R.T.; Brassell, S.C.; Eglinton, G. Organic geochemical indicators of palaeoenvironmental conditions of sedimentation. *Nature* **1978**, *272*, 216–222. [CrossRef]
67. Ten Haven, H.L.; De Leeuw, J.W.; Rullkötter, J.; Damsté, J.S. Restricted utility of the pristane/phytane ratio as a palaeoenvironmental indicator. *Nature* **1987**, *330*, 641–643. [CrossRef]
68. Fathy, D.; El-Balkiemy, A.F.; Makled, W.A.; Hosny, A.M. Organic geochemical signals of Paleozoic rocks in the southern Tethys, Siwa basin, Egypt: Implications for source rock characterization and petroleum system. *Phys. Chem. Earth Parts A/B/C* **2023**, *130*, 103393. [CrossRef]
69. Peters, K.E.; Cassa, M.R. Applied source rock geochemistry. In *The Petroleum System: From Source to Trap*, 2nd ed.; Magoon, L.B., Dow, W.G., Eds.; AAPG Memoir: Tulsa, OK, USA, 1994; Volume 60, pp. 93–120.
70. Hughes, W.B.; Holba, A.G.; Dzou, L.I.P. The ratios of dibenzothiophene to phenanthrene and pristane to phytane as indicators of depositional environment and lithology of petroleum source rocks. *Geochim. Cosmochim. Acta.* **1995**, *59*, 3581–3598. [CrossRef]
71. Law, C.A. Evaluating Source Rocks. In *Treatise of Petroleum Geology/Handbook of Petroleum Geology: Exploring for Oil and Gas Traps*, 2nd ed.; Edward, A.B., Norman, H.F., Eds.; AAPG: Tulsa, OK, USA, 1999; pp. 6–41.
72. Kelts, K. Environments of deposition of lacustrine petroleum source rocks: An introduction. In *Lacustrine Petroleum Source Rocks. Geological Society Special Publication No. 40*, 2nd ed.; Fleet, A.J., Kelts, K., Talbot, M.R., Eds.; Blackwell Scientific Publications: Oxford, UK, 1988; pp. 3–26.
73. Vandenbroucke, M.; Largeau, C. Kerogen origin, evolution and structure. *Org. Geochem.* **2007**, *38*, 719–833. [CrossRef]
74. Chen, Z.H.; Huang, W.; Liu, Q.; Zhang, L.Y.; Zhang, S.C. Geochemical characteristics of the Paleogene shales in the Dongying depression, eastern China. *Mar. Petrol. Geol.* **2016**, *73*, 249–270. [CrossRef]
75. Ma, B.B.; Cao, Y.C.; Eriksson, K.A.; Jia, Y.C.; Wang, Y.Z. Burial evolution of evaporites with implications for sublacustrine fan reservoir quality: A case study from the Eocene Es4x interval, Dongying depression, Bohai Bay Basin, China. *Mar. Petrol. Geol.* **2016**, *76*, 98–114. [CrossRef]
76. Hussain, M.; Warren, J.K. Source rock potential of shalww-water evapqprltes: An investigation in holocenepleistocene salt flat sabkah (playa), west texas-new mexico. *Carbonate Evaporite* **1991**, *6*, 217–223. [CrossRef]
77. Sinninghe Damste, J.S.; Kenig, F.; Koopmans, F.P.; Koster, J.; Schouten, S.; Hayes, J.M.; de Leeuw, J.W. Evidence for gammacerane as an indicator of water column stratification. *Geochem. Cosmochim. Acta* **1995**, *59*, 1895–1900. [CrossRef]
78. Alkhafaji, M.W.; Aljubouri, Z.A.; Aldobouni, I.A. Depositional environment of the Lower Silurian Akkas hot shales in the Western Desert of Iraq: Results from an organic geochemical study. *Mar. Petrol. Geol.* **2015**, *64*, 294–303. [CrossRef]
79. Banerjee, A.; Sinha, A.K.; Jain, A.K.; Thomas, N.J.; Misra, K.N.; Chandra, K. A mathematical representation of Rock-Eval hydrogen index vs. T_{max} profiles. *Org. Geochem.* **1998**, *28*, 43–55. [CrossRef]

80. Hao, F.; Chen, J.Y. The cause and mechanism of vitrinite reflectance anomalies. *J. Petrol. Geol.* **1992**, *15*, 419–434.
81. Hao, F.; Zou, H.; Gong, Z.; Yang, S.; Zeng, Z. Hierarchies of overpressure retardation of organic matter maturation: Case studies from petroleum basins in China. *AAPG Bull.* **2007**, *91*, 1467–1498. [CrossRef]
82. Liu, H.; Cao, Y.; Jiang, Z.; Wang, S.; Wang, Y.; Xu, L. Distribution characteristics of evaporites and formation pressure of the fourth member of the Shahejie Formation in the Dongying depression, the Bohai Bay Basin. *Oil Gas Geol.* **2009**, *30*, 287–293.

Disclaimer/Publisher's Note: The statements, opinions and data contained in all publications are solely those of the individual author(s) and contributor(s) and not of MDPI and/or the editor(s). MDPI and/or the editor(s) disclaim responsibility for any injury to people or property resulting from any ideas, methods, instructions or products referred to in the content.